Egyptian Journal of Chemistry

http://ejchem.journals.ekb.eg/

Synthesis, Characterization (Theoretical and Biological Study) of Some Transition Metal Complexes with New Schiff Base Derived from 1,2,4-triazole

Mahmoud Najim AL-Jibouri*[a], Waleed A. Jawad[b], Asim A. Balakit[c] and Mohammed Obies[c]

[a] *Department of Chemistry, College of Science, Mustansiriyah University, Baghdad-Iraq*
[b] *Ministry of Education, Babylon Education Directorate, Hilla-Iraq*
[c] *College of Pharmacy, University of Babylon, Hilla-Iraq*

Abstract

The present work involves, new Schiff base of (E)-2-(((3-mercapto-5-(3,4,5-trimethoxyphenyl)-4H-1,2,4-triazol-4-yl)imino)methyl)phenol (L_2) has been synthesized by condensation reaction of 4-amino-5-(3,4,5 trimethoxy phenyl)-4H-1,2,4-triazole-3-thiol with 2-hydroxybenzaldehyde. The new Schiff base (L_2) used as a ligand to synthesize a new complex with Co(II), Ni(II), Cu(II), Pd(II), and Cd(II) metal ions by 1:1 (Metal: ligand) ratio. New ligand and their complexes have been exanimated and confirmed by fourier-transform infrared (FT-IR), ultraviolet-visible (UV-visible), proton nuclear magnetic resonance (^{1}HNMR), carbon13 nuclear magnetic resonance (^{13}CNMR), microelement analysis (CHNS), thermal analysis (TG-DSC), atomic absorption flame (AAF), conductivity and magnetic susceptibility. The results obtained from spectra, elemental analyses and thermal analyses (TG-DSC) and compare by density functional theory (DFT) and TD-DFT calculations were screened for some selected complexes and the observed data indicated their stability and the expected chemical formula, Pd(II) were square planner, whereas the Cu(II), Co(II), Ni(II) octahedral, and Cd(II) were tetrahedral geometry . Furthermore, the antibacterial and antifungal activity was screened for the DMSO solution concerning the Schiff base (L_2) and its complexes (20 µg/ml) against two kinds of gram; (*Staphylococcus aureas* and *Bacillus subtilis)* positive and two negative bacteria; (*Esherichia coli* and *Burkholderia*) and against (*Candida albican)* fungi. The results obtained from diffusion method confirmed the greater activity of Pd(II) and Cd(II) complexes whereas the Co(II),Cu(II) and Ni(II) complexes showed medium activity compared with the low inhibition zones of the free Schiff base of 1, 2, 4- triazole derivative.

Keywords: Schiff base derived from 1,2,4-triazole, metal Complexes, Theoretical studies, Biological activity of ligand and its complexes.

1. Introduction

The 1,2,4-triazole derivatives belong to the five-membered heterocyclic family composed of three atoms of nitrogen and mainly occurs in various isomeric forms: 1,2,3-triazole and 1,2,4-triazole [1, 2]. The literature studies about 1,2,4-triazole containing derivatives have exhibited a variety of such bioactivities, as an antimicrobial agent [3], antitubercular agent [4], anticancer agent [5,6], anticonvulsant agent [7], anti-inflammatory agent [8]. It has been documented that Schiff bases, a significant class of organic compounds, have a broad spectrum of activities. Schiff based derived from 1,2,4-triazoles have highly significant biological activities such as anti-inflammatory, antibacterial, antioxidant, antifungal , anticancer, antimarial , anticonvulsant [9] and are thus an interesting field of research for these compounds. Furthermore, the thiol-thione tautomer's of 1,2,4-triazoles[10]. 1,2,4 triazole derivatives obtained by the thiol form are less frequent than the Mannich bases obtained by the thione form [11]. The ligand derived from bis (4-amino-5-mercapto-1,2,4-triazol-3-yl) alkanes are considered to be good coordinating ligands, the ligands are tetra dentate coordination to the metal ions through sulphur and amine group [12]. There are studies of the coordination behavior of a Schiff base with SNO donation sites, derived from 4-amino-5-phenyl-4H-

*Corresponding author e-mail: Mahmoud_inor71@uomustansiriyah.edu.iq.; (Mahmoud Najim AL-Jibouri).
Receive Date: 10 April 2021, Revise Date: 02 May 2021, Accept Date: 04 May 2021
DOI: 10.21608/EJCHEM.2021.71885.3580

1,2,4-triazole-3-thiol and salicaldehyde condensation, against certain bi- and trivalent metal ions, namely chrome(III), manganese(II), iron(III), cobalt(II), copper(II) and zinc(II). The chelates were found to have octahedral, trigon bi pyramidal and tetrahedral structures [13]. The poly dentate Schiff bases that are possessing triazole ring have interested wide scope of applications in the antioxidants and anticancer fields [14,15].In the view of the varied applications and significances of triazole ligands and their coordination compounds, we decided to prepared new Schiff base ligand (L_2) (E)-2-(((3-mercapto-5-(3,4,5-trimethoxy phenyl)-4H-1,2,4-triazol-4-yl) imino)methyl)phenol) with selected metals complexes Cu (II), Ni(II), Pd (II), Cd(II) and Co (II) and their computational studies.

2. Experimental

All the chemicals from Sigma-Aldrich and Fluka were used in this study.

2.1. Synthesis of 3,4,5-Trimethoxybenzoic acid (S1)

Gallic acid mono hydrate was added to a cold solution of (40 gm, 1.0 moles) of sodium hydroxide in (250 ml) water in a 3-neck round bottom flask (25 gm , 0.133 mole). The flask is closely stopped immediately and the mixture is periodically mixed until all of the acid has dissolved. Dimethyl sulfate (0.36 mole , 33 ml) was added and the flask was stirred for this reason (20 minutes). In order to prevent the temperature from increasing above (30-35) °C, the mixture was kept cold. To release some pressure, the cover is occasionally lifted. A second similar volume of di methyl sulfate was added and stirring continued for a greater range of (20 minutes). The temperature will increase to (40-45) ° C during this second addition. The flask is then fitted with a reflux condenser and the contents are cooked for two hours by stirring. A solution of (10 gm) sodium hydroxide is then added to (15 ml) of water and the boiling continues for an additional two hours. The reaction mixture is then cooled and (5 percent) diluted hydrochloric acid is acidified. The precipitated is filtered with suction and washed well with cold water and recrystallized from ethanol to give compound (S1)scheme.1[15] Color (brown crystal),Yield (85%), M.p (170-172)°C, M.wt (212 gm/mol), FT-IR (KBr,cm^{-1}):broad bend υ(O-H) (3020-2516), υ (C=O) acid (1681) , υ C-H aliph.(2945 and 2836).

2.2. Synthesis of 3,4,5-Trimethoxymethylbenzoate (S2)

Sulfuric acid (1.5 ml) was added dropwise to the mixture of compound (S1) (10.6 gm,0.05 mole) in methanol (30 ml). For 8 hours, the mixture was heated under reflux, the reaction was controlled using thin-layer chromatography (TLC). After cooling, the precipitate formed. The methanol excess was evaporated and the solid product was washed with a solution of sodium bicarbonate , filtered, washed with cold water, dried and recrystallized from ethanol to give compound (S2) Scheme1[16]: Color (white crystal), Yield (95%), M.p (83-85)°C, M.wt (226 gm/mol), Rf = 0.87(ethylacetate : chloroform ,1:2). FT-IR (KBr,cm-1): υ(C=O)ester(1713), υC-H Ar-3079), υC-H aliph (2951).

2.3. Synthesis of 3,4,5-Trimethoxybenzohydrazide (S3)

To the solution of compound (S2) (9 gm., 0.04 mole) in (40 ml) of absolute ethanol, hydrazine hydrate (80 % ,15 ml) was added. The mixture was refluxed for 14 hours, the reaction was controlled using thin-layer chromatography (TLC) and then mixture was allowed to cool down . A solid product was filtered, washed with cold water, dried and recrystallized from ethanol to give compound (S3) Scheme.1[17]: Color (white) , Yield (90%), M.p (160-163)°C, M.wt (226 gm/mol), R_f = 0.25 (ethylacetate : chloroform , 1:2). FT-IR (KBr ,cm^{-1}): υ(NH_2) asym. and sym. (3366 and 3334), υ(NH) (3292), υ(C=O) amide (1651), υC-H arom. (3010), υ C-H aliph (2938).

2.4. Synthesis of potassium-2-(3,4,5-tri methoxy benzoyl) hydrazine carbodithioate (S4)

Compound (S3) (4.5 gm., 0.0195 mole) was treated with a solution of potassium hydroxide (1.8 gm., 0.0321 mole) in methanol (35 ml) at 0°C with stirring, then (0.2mole ,7 ml) of carbon disulfide was added dropwise and the reaction mixture was stirred overnight at room temperature. And then added (100 ml) diethyl ether to cool the reaction with stirred for 10 minutes. The solid product was filtered , washed with cold methanol and dried to give compound (S4) Scheme.1[18]: Color (pale yellow powder), Yield (95%), M.p (225-227)°C , M.wt (340 gm/mol), FT-IR (KBr,cm^{-1}): υ(NH) (3275-3223), υ(C=O)amide (1649) , υ(C=S)(1262),υC-H arom.(2998), υC-H aliph (2939).

2.5. Synthesis of 4-Amino-5-(3,4,5-Trimethoxiy phenyl)-4H-1,2,4-triazole-3-thion(L_1)

A mixture of compound (S4) (4.5 gm, 0.0132 mole) in excess amount of hydrazine hydrate (about 25 ml) was heated under reflux for 6 hrs. A color change of mixture from black green into light yellow , this is to release hydrogen sulfide gas by changing the lead acetate sheet from black to white, the reaction was controlled using thin-layer chromatography (TLC) . The cooled mixture was poured into ice–water (30 ml) and acidified with conc. hydrochloric acid pH = 2-3 . The precipitate was filtered , washed with cold water, dried and recrystallized from ethanol to give

compound (L_1) Scheme1 [19]: Color (white powder) ,Yield (55%) ,M.p (214-216)°C, M.wt (282 gm/ mol), R_f = 0.5 (ethylacetate : chloroform , 1:2). FT-IR (KBr ,cm^{-1}) :υ(NH_2) asym. and sym.(3300 and 3247), υ(NH) (3189), υ(S-H) (2728), υ(C=S) (1237) .^{1}H NMR (400 MHz, CDCl3, δ ppm): 10.45 (S, Week,SH), 7.46 (S, 2H, aromatic), 4.89 (S, broad ,NH2) 3.9 (S,6H, 2OCH3), 3.8 (S, 3H, OCH3) , ^{13}C NMR (100-MH_Z, DMSO) 56.60, 56.65, 60.64, 105.77, 121.43, 139.88 , 153.28 , 167.09 . MS (*m/z* %): 281.1 [M+].

2.6. *Synthesis of the schiff base ligand (E)-2-(((3-mercapto-5-(3,4,5-trimethoxyphenyl)-4H-1,2,4-triazol-4-yl)imino)methyl)phenol (L_2)*

A hot solution of (L_2) equimolar quantity (0.001 mol, 0.282 gm.) was added slowly and drop-wise into a solution of salicyaldehyde (0.001 mol, 0.122 gm.) in the presence of (5-6) drops of glacial acetic acid, and the mixture was refluxed for 6 hours, the reaction was controlled using thin-layer chromatography (TLC) , allowed to cool over-night at room temperature. The precipitate was filtered and washed with hot ethanol absolute, then dried in the air to obtain the ligand (L_2) scheme1 [20].Color (yellow crystal),Yield (72%), M.p (222-225),°C, M.wt (386 gm/ mol), R_f = 0.33 (ethylacetate : n-hexane, 1:2).FT-IR (KBr,cm^{-1}):υ(OH phenol)(3229), υ(S-H) (2712), υ(C=N)(1624).^{1}HNMR (400 MHz, CDCl3, δ ppm): 10.55 (S,1H,OH), 9.79 (S,1H,CH=N),7.10(S,2H,aromatic),6.53(d,1H,aromatic), 7.29(d, 1H, aromatic), 6.61 (t, 1H, aromatic), 7.38 (t,1H,aromatic),3.89(S,6H,2OCH3),3.94(S,3H,OCH3). ^{13}CNMR (100MH_Z,CDCl3) 56.25, 105.76, 117.18, 117.31, 119.74, 132.57, 133.45, 143.52, 153.58, 159.83, 164.7.

2.7. *Synthesis of the solid metal complexes of (1-5)*

Complexes were synthesized by dissolving (1 m mole, 0.386 gm.) (L_2) in hot solution (20 mL) (DMF: ethanol in 1:1) and mixing (20 mL, 1 m mole) with hot ethanol of the metal ion ($CoCl_2$.6H2O, $CuCl_2.2H_2O$, $NiCl_2.4H_2O$, $CdCl_2.2H_2O$ and $PdCl_2$ in (1:1) as a ratio of metal to ligand in accordance with scheme 2. The mixture left them under reflux for (10-12) hrs and then allowed the solid complexes to be cooled and added (10 mL) of diethyl ether to precipitate. They filtered the crystals, washed them with cold water, ethanol and dried them. Table1 represents the percentage yield and physical characteristics of the ligand (L_2) and its complexes [21].

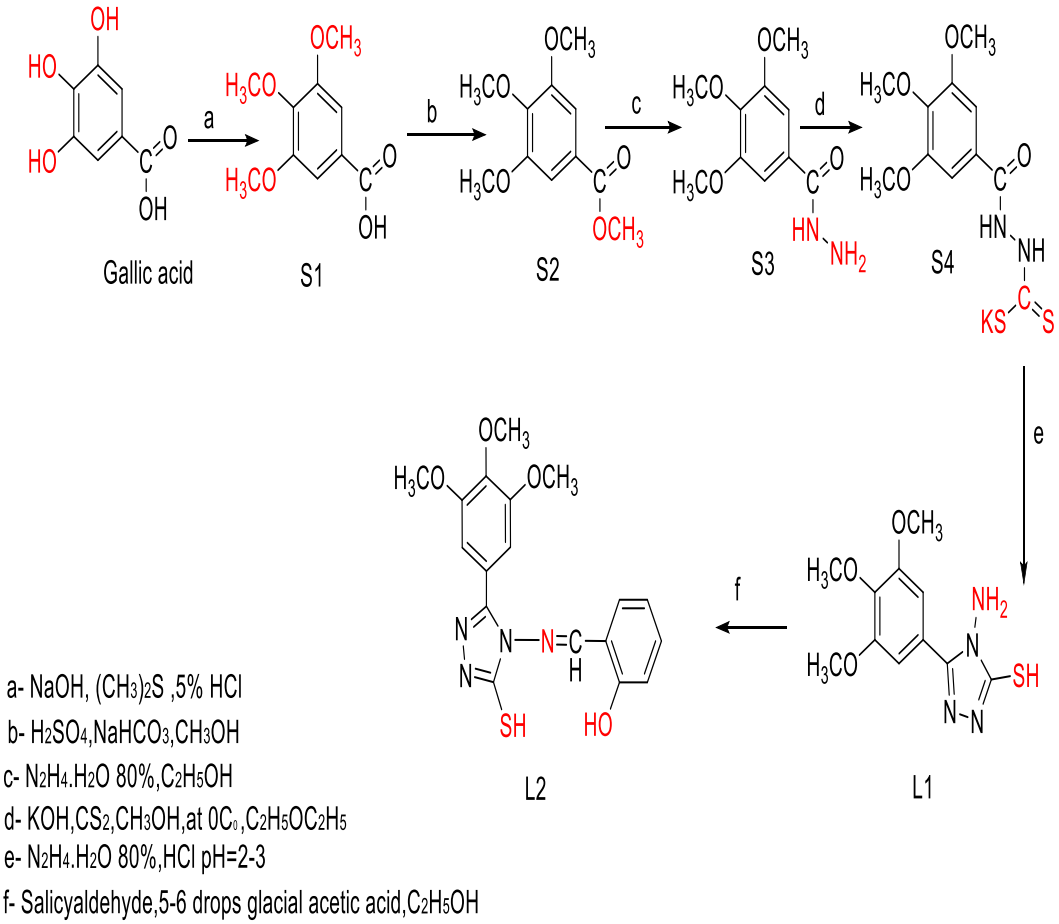

Scheme 1. synthesis of the schiff base ligand (L_2) : (E)-2-(((3-mercapto-5-(3,4,5-trimethoxyphenyl)-4H-1,2,4-triazol-4-yl)imino)methyl)phenol

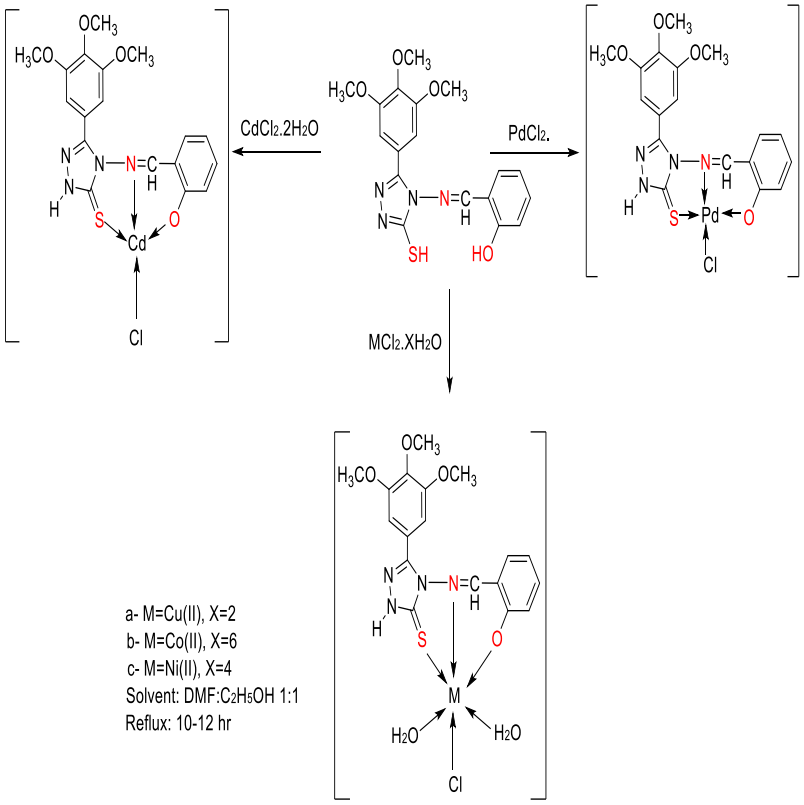

Scheme 2. Synthesis of the solid metal complexes

2.8. Computational methods

All DFT calculations in this paper were done with ORCA package [22]. Two functionals for geometry optimization were used in this work, the BP86 [23-24], and B3LYP functional [25,26], with the atom-pairwise dispersion correction with the Becke-Johnson damping scheme (D3-BJ)[27,28]. The def2-SVP [29] basis set were used for all atoms except the transition metal center (Cu(II), Co(II), Ni(II), Pd(II), and Cd(II) where def2-TZVP is used. The RI approximation was used with the def2/J auxiliary basis. Relativistic scalar ZORA [30] is used on the top of basis set of the second raw transition metals (Pd and Cd). TD-DFT calculations were performed in the Tamm-Dancoff approximation using M06-L functional [31].

2.9. Antifungal Activity

The anti-fungal and antibacterial study was applied against *Candida albicans* by agar diffusion method and grown the fungi strain on potato dextrose at (37Ċ) for (48 hour), we used fluconazole as reference antifungal drug with DMSO solvent was used as negative control to determine the inhibition zone against *Candida albicans* .The free Schiff base (L2) and its metal complexes were studied antibacterial activity in the concentration (20 µg/ml) in DMSO against two kind of bacteria , two gram positive bacteria (*staphylococcus aureas, Bacillus subtilis)* and two gram negative bacteria (*Esherichia coli, Burkholderia)*.The method of agar diffusion was used to determine the inhibition zone in (mm) units for antibacterial, the storage of the bacteria strains was done in Muell or Hinton broth and were subcultures for testing compound in the same medium and growth at (37Ċ).The stock solutions of the tested ligands complexes in DMSO and the concentration was (20 µg/ml), the dilutions method were applied according to guide lines at national committees for clinical standard 1997 [46], As well as the pH of the solution was adjusted to (7.5) by NaOH drop (concentrate = 2%). The resulting solutions were Autoclave for (45 min) and completing the volume of solution of nutrient agar in order to be steady in petri plates, the measuring of diameter zones (mm) of the inhibition was measured according to the procedure described in literatures [47].

3. Results and Discussion

Table 2 shows the physical measurements and chemical characteristics of the schiff base ligands and their metal complexes. Based on C.H.N.S, flam atomic absorption, conductivity measurements and magnetic susceptibility and spectral results, the molecular formulae of studied compounds were suggested. The data shows the formation of 1:1 (ligand: metal) ratio complexes. The knowledge clearly shows that the used

ligand acts as a neutral tridentate. In common organic solvents, the complexes are insoluble, but all the complexes are fully soluble in DMF and DMSO. The complexes of synthesized metals (II) are air-stable, microcrystalline solids.

3.1. FT-IR *Study*

The FT-IR spectrum characterized a new schiff base ligand L_2 and its complexes Table 1,Figures (1, 2). The result show exhibited new bands at 3229, 2712 ,1624 and (1421) cm^{-1} indicating the vibration modes υ(OH phenolic), υ(S-H), υ(CH=N) , υ(C=S) respectively . The comparison of ligand spectrum with FT-IR spectra of all prepared metal complexes, The shift of υ(C=S) and υ(C=N) imine in their positions and change the shape or intensity of band compared with the ligand (L_2) attributable to the coordination of this ligand with the metal ions, and gave an indication that the complexes were formed , also the absorptions band of υ(OH phenolic) group disappearance , these remarkable changes would have give strong evidences for the active sites of imine moiety and oxygen leading to stable six-member ring up on chelation. The observed absorptions at around (1619-1614) cm^{-1} and (1211-1235) cm^{-1} and a singlet at (3160) cm^{-1} confirming the shift in tautomers forms with (N2-H). The results of IR spectra concluded that the Schiff base, (L_2) behaves as mono basic tridentate ligand through nitrogen of azomethine group υ (CH=N), υ(OH phenolic) and thione group υ(C=S). However, the new weak bands at υ(550-200) cm^{-1} which are associated with υ(M-N), υ(M-S), υ(M-O) and υ(M-Cl) coordination bonds [32,33].

Table 1: FT-IR data of new Schiff base ligand and their complexes

NO	υ(CH=N)	υ(O-H)	υ(C=S)	(M-N)	(M-S)	(M-O)	(M-Cl)
L_2	1624	3229	1238	-	-	-	-
1	1617	-	1235	549	455	347	312
2	1615	-	1230	503	458	384	368
3	1619	-	1235	504	452	365	319
4	1614	-	1222	529	465	336	316
5	1617	-	1211	502	453	375	310

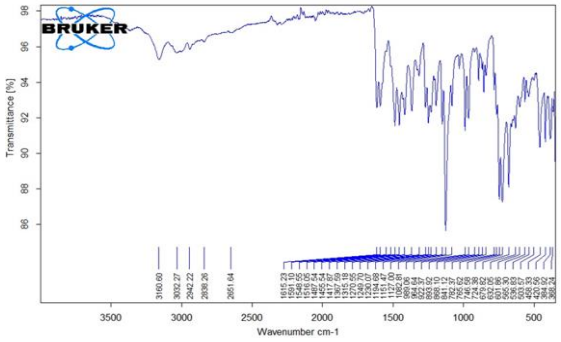

Fig.1.FT-IR spectrum of Schiff base ligand (L_2)

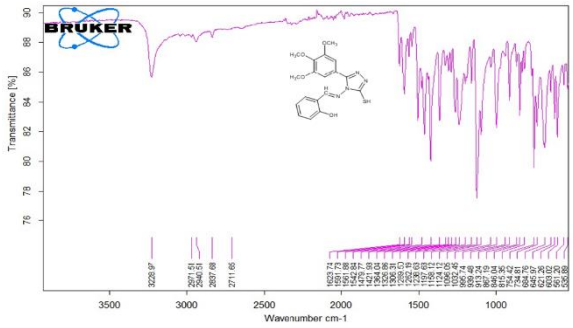

Fig. 2. FT-IR Spectrum of metal complex CuL_2

Table 2. Physical properties and analytical data of the Schiff base ligand (L_2) and its metal complexes.

No	Compound	Color	M.wt	Yield%	M.p c°	Micro Elemental Analysis Found (calc.)				Metal content Found (calc.)
						C%	N%	H%	S%	
L2	$C_{18}H_{18}N_4O_4S$	yellow	386	72	222-225	(55.8) 53.05	(14.5) 13.58	(4.66) 3.56	(8.28) 7.49	-
1	$[Ni(L_2)(H_2O)_2Cl]$	pale yellow	515.6	58	233-235	(41.89) 41.98	(10.86) 10.78	(4.26) 4.34	(6.20) 6.98	(11.38) 10.91
2	$[Cu(L_2)(H_2O)_2Cl]$	dark green	520.4	71	280 dec	(41.50) 42.30	(10.76) 10.43	(4.22) 3.13	(6.14) 5.27	(12.20)11.23
3	$[Co(L_2)(H_2O)_2Cl].H_2O$	pale yellow	533.8	61	235-238	(40.46) 40.78	(10.49) 10.34	(4.49) 4.55	(5.99) 5.37	(11.42)12.54
4	$[Pd(L_2Cl]$	brown	527.3	66	245-247	(40.96) 40.54	(10.62) 10.78	(3.41) 3.36	(6.06) 5.43	(20.17)19.7
5	$[Cd(L_2Cl]$	orange	533.3	56	252-254	(40.50) 40.32	(10.50) 10.41	(3.37) 3.21	(6.00) 5.49	(21.07)20.86

3.2 NMR and Mass Spectra Studies

The ^{1}H-NMR compound spectrum (L_1), Figure (3), showed four singlet signals at δ = 3.8, 3.9, 4.89 and 7.46 ppm corresponding to the protons (pOCH3, 2mOCH3, NH2 and aromatic group) respectively, the singlet peak at δ = 10.45 ppm corresponding to the state (SH-NH tautomeric). In addition, ^{13}C-NMR spectra, Figure 4 showed eight signals at 56.60 ppm duo to (2C symmetrical C17, 19) and 60.64 ppm due to (C15), 105.77ppm due to (2C symmetrical C3,5), 125.86 ppm due to (C4), 139.88 ppm due to (C1), 149.63 ppm due to(2C symmetrical C2,6), 153.28 ppm due to (C7) and 167.09 ppm due to (C9). The mass range, which corresponds to the molecular weight of the structure assigned to this compound Figure (5) , gives a high intense molecular ion peak at m/z= 281 in addition to the following expected fragments 223, 135, 79, 28 m/z. The some significant fragmentation ions of this compound are shown in scheme 3, [34].

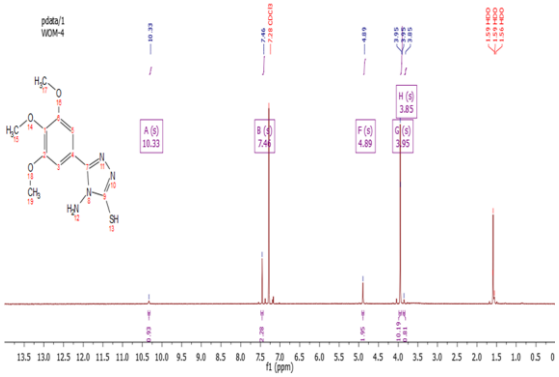

Fig 3. ^{1}H-NMR spectrum for Compound (L_1)

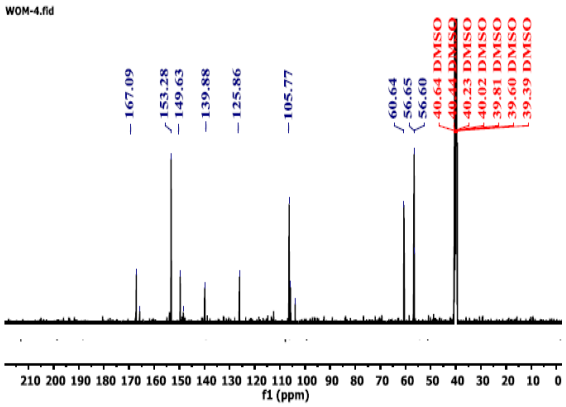

Fig 4. ^{13}C-NMR spectrum for Compound (L_1)

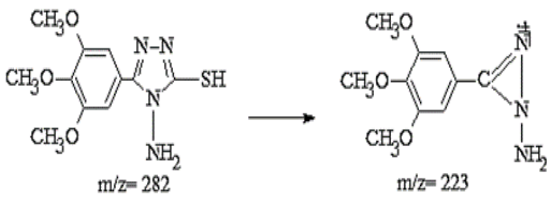

Scheme 3. Mass fragmentation ion of compound (L1)

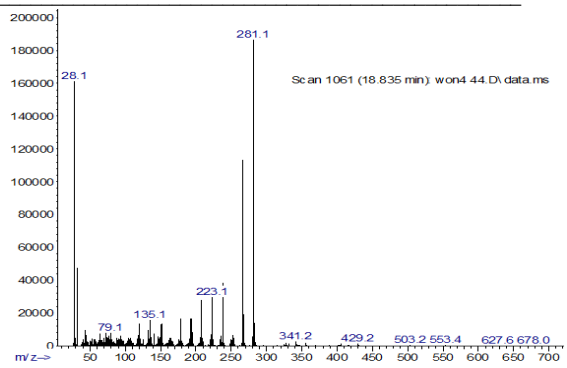

Fig 5. Mass spectrum for Compound (L1)

Furthermore, the Schiff base ligand (L_2) was fully characterized by ^{1}H-NMR and ^{13}C-NMR. The Figure (6), showed ten signals at δ = 3.89 and 3.94 corresponding to the protons (2mOCH3, pOCH3) respectively, the singlet peak at δ = 10.55 ppm corresponding to the protons (OH) while the singlet peak of (SH-NH tautomeric) does not appear. As well as is very important the singlet peak at δ = 9.79 ppm du to proton (CH=N) to avoidance consist Schiff base ligand, in addition the nuclear resonance of aromatic protons Ar-H were recorded different signals about (6.53-7.38) ppm, ^{13}C-NMR spectra, Figure (7) showed 14 signals at 56.25 ppm due to (C23) and 59.28 symmetrical 2C 25, 27) 105.76 ppm due to (symmetrical 2C 3, 5) ,117.18 ppm due to (C 15, C19), 117.31 ppm due to (C17), 119.74 ppm due to (C16) 131.76 ppm (C18), 132.57 ppm due to (C1), 133.45 due to (C7), 143.52 ppm due to (symmetrical 2C 2,6), 153.58 ppm due to (C4), 159.83 ppm due to (C14), 161.57 ppm (C 9), 164.7 ppm due to (C20). The mass range, which corresponds to the molecular weight of the structure assigned to this compound, gives a high intense molecular ion peak at m/z = 386, and the base ions of this compound are shown at m/z= 119.

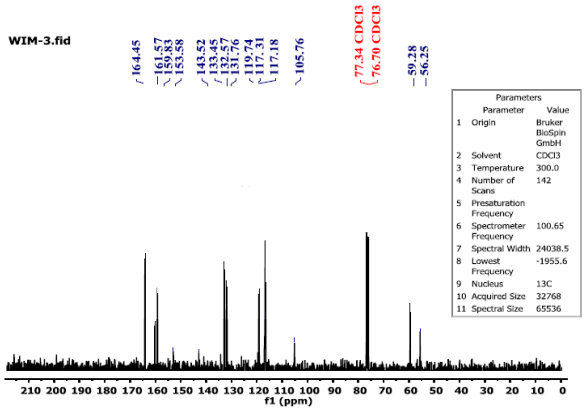

Fig 6. 1H-NMR spectrum for Schiff base ligand (L2)

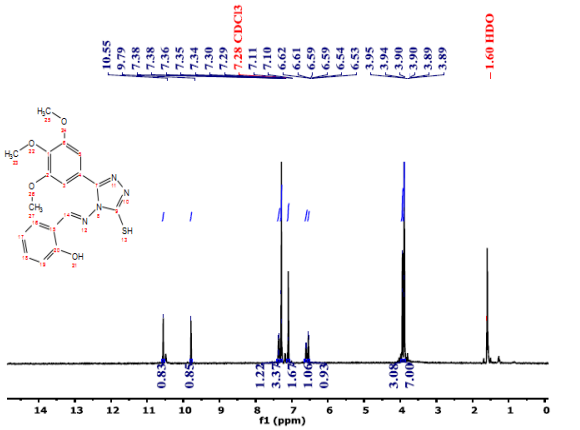

Fig 7. 13C-NMR spectrum for Schiff base ligand (L_2)

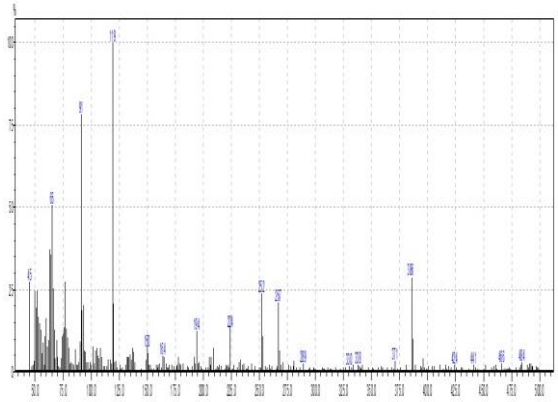

Fig 8. Mass spectrum for Schiff base ligand(L_2)

3.3 Molar Conductance, Electronic Spectra and Magnetic Properties

The complexes molar conductance values measured at room temperature in DMF solution with a concentration of 0.001 mol/L fall within the 2-5 $ohm^{-1}.cm^2.mol^{-1}$ range Table 3, indicating the non-electrolytic nature of the complexes assigning to absence of chloride ions as counter ion in the structure of complexes. It was, however, determined that chloride ion outside the coordination sphere by adding a silver nitrate solution lead to not precipitate AgCl [35]. The electronic absorption spectra of the metal complexes were recorded in DMSO at room temperature and the result are listed in Table 3. The yellow solution of ligand in ethanol exhibited four peaks at around 28248 cm^{-1} assigned to (n–π*) transition and 34246, 39062 and 46672 cm^{-1} were assigned to (π-π*) transitions [36]. The pale yellow solution of Ni (II) complex exhibited three spin-allowed absorptions at 10405 and 23255 cm^{-1} are assigned to $\upsilon_1 = {}^3A_2g \rightarrow {}^3T_2g$ (F),$\upsilon_2 = {}^3A_2g \rightarrow {}^3T_1g$ (F) while the third transition of $\upsilon_3 = {}^3A_2g \rightarrow {}^3T_1g$ (P)[37] was obscured due to the high intensity band of LMCT at around 33444.81 cm^{-1} with extinction coefficient (Є=2500 $L.cm^{-1}$/mole) of nickel(II). Based on the Tanabe-Sugano diagram of $3d^8$ configuration regarding octahedral complexes of nickel (II). The intercepts on y-axis which represents the (E/B) value is 35, the average Racah parameter (B) is equal 550 cm^{-1}. As well as the intercept on x-axis (x=38) ; the splitting energy will be equal 16550 cm^{-1} which is in well agreement of 10Dq of nickel (II) complexes. The magnetic moment value of 2.8 B.M for Ni (II) complexes corresponds to two unpaired electrons and octahedral geometry. By the same way low-spin state of Pd (II) complex that it showed two spin-allowed absorptions at 22727 and 28571 cm^{-1} assigned to $\upsilon_1 = {}^1A_1g \rightarrow {}^1T_1g$ and $\upsilon_2 = {}^1A_1g \rightarrow {}^1T_1g$ (G) respectively [38]. The ratio of $\upsilon_2/\ \upsilon_1$=1.257 and from T-S diagram Δ_{oct}/B of 35 yields E/*B* values of 35 and 38. The Racah parameter (B) is equal 649.34 and 751.86 and the average (B) =700.6 cm^{-1}. From the x value the Δ_{oct}/B = 29, it is equal 20317.522 cm^{-1} which is confirming the data observed from literature for low spin square planner of Pd (II) complexes, and the diamagnetic moment of Pd (II) complexes, all electrons are paired. As well as the yellow solution of Co (II) complex showed two spin-allowed transitions at 23809 and 25706 cm^{-1} which are associated with $\upsilon_1 = {}^2Eg \rightarrow {}^2T_2g$ (F), $\upsilon_2 = {}^2Eg \rightarrow {}^1T_1g$ (F) respectively [39], since the term ground symbol in its low-spin state of ($t_2g^6\ eg^1$) is ^2G with ground state ^2E_g according to T-S diagrams. The calculated of Racah parameter and splitting energy are 680 and 25200 cm^{-1} .The magnetic moment values of 1.98 B.M. for Co (II) complexes undoubtedly suggest low spin octahedral geometry with one unpaired electron for Co (II) complexes, that are strong evidence for the strong field of poly dentate ligands of triazole derivatives. The dark green solution of Cu (II) complex showed shoulder peak at 13333 cm^{-1} and other at 23585 cm^{-1} which are attributed to $^2Eg \rightarrow {}^2T_2g$, LMCT respectively [40]. The magnetic moment values of 1.78 B.M. for Cu (II) complexes depending on all previously mentioned results we can suggest distorted octahedral geometry. The off white solution of Cd (II) complex showed high intensity bands at around 28011, 33575 and 44843 cm^{-1} are associated with MLCT and ligand spectra of –C=S, -C=N and –C=C chromophres, according to these results we can suggest an tetrahedral geometry [41].

Table 3: Conductivity, Magnetic and Electronic spectra of metal complexes 1–5

No	λ_{max}nm (υ cm^{-1})	Assignment	ohm^{-1}.cm^2.mol^{-1}	μ B.M. found (calc)	Suggested Structure
L_2	354 (28248)	n → π*	-	-	-
	292 (34246)	π → π*			
	256 (39062)	π → π*			
	214 (46672)	π → π*			
1	961 (10405)	$^3A_2g \rightarrow {}^3T_2g$ (F)	3.6	2.0	Octahedral
	430 (23255)	$^3A_2g \rightarrow {}^3T_1g$ (F)		(2.4)	
	299 (33444)	LMCT			
2	750 (13333)	$^2Eg \rightarrow {}^2T_2g$	5.1	1.78	Octahedral
	424 (23585)	LMCT		(1.73)	
3	420 (23809)	$^2Eg \rightarrow {}^2T_2g$ (F)	3.5	1.98	Octahedral
	389 (25706)	$^2Eg \rightarrow {}^1T_1g$ (F)		(1.73)	
4	440 (22727)	$^1A_1g \rightarrow {}^1T_1g$ $^1A_1g \rightarrow {}^1T_1g$	3.0	Dia	Square planer
	350 (28571)	(G)			
5	375 (28011)	MLCT	2.9	Dia	Tetrahedral
	295 (33575)	n → π*			
	245 (44843)	π → π*			

3.4 Thermo gravimetric analysis of Ligand and CuL2 *Complex*

Thermogravimetric analyses were performed under di nitrogen N_2 atmosphere at the heating rate of 6.2℃ min^{-1} of the complexe. The thermal stability of Schiff based ligand (L_2) were confirmed beside their chemical formula elucidation. The TG-DSC of (L_2) ligand exhibits exothermic fragmentation at 211℃ with % weigh loss 8.6 and the differential DSC cure was optimized at 259℃. As well as the second and third steps of thermal analysis was observed at 415℃ and 555 ℃ with % weight losses at around (4.7-5.5) respectively. These fragmentations can be attributed to the breakdown of the weak points in the structure of ligand like trimethoxy phenyl groups. However, the DSC curve at maximum temperature T_{max} = 610℃ confirms the thermal stability of the ligand through the immine –C=N-,hydrogen bonded –OH and thioamide C=N-SH with HN=C=S forms respectively, Figure 9.

The TG-DSC of CuL_2 in N2 atmosphere, Figure 10, exhibits TG curve at (190-220) ℃ with loss weight =10% which is associated with the cleavage of coordinated water molecules in the inner-sphere of complex. The second step of TG was shown at (300-320) ℃ range with loss weight=8.5% which is ascribed to break down of weak points of complex like –OCH3 and phenyl groups [42]. As well as the TG curve observed at (400-415) ℃ temperature may be assigned to break down of –Cl and rest organic triazole ring with stable phase of CuO with 55% weight value.

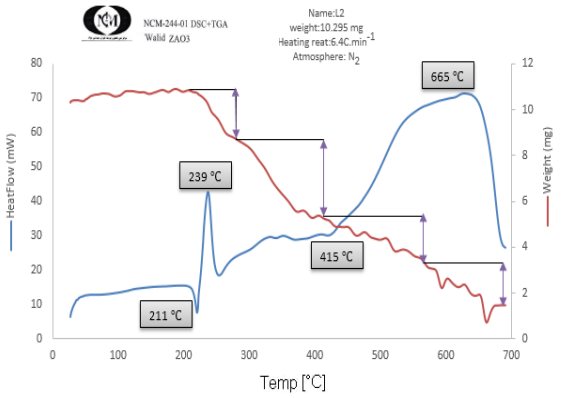

Fig 9. TG-DSC of Schiff base ligand (L_2)

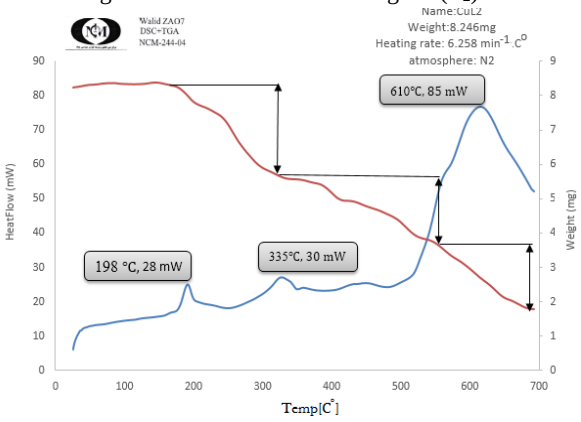

Fig 10. TG-DSC of metal complex CuL_2

3.5 Computational Study

The geometries of the Cu(II), Pd(II), Co(II), Cd(II), and Ni(II) complexes were suggested based on electronic spectra, elements analyses, and the thermal analyses methods. However, these methodologies give no information about structure parameters such as bond lengths and bond angles, therefore, density

functional theory (DFT) calculations were carried out to gain insight into these parameters. In the DFT calculations we have applied two quite different exchange-correlation functionals that are BP86 and B3LYP. Geometry optimizations were carried out for all possible spin states within the 3/4d-orbital, ^{2}A for Cu (II), ^{1}A and ^{3}A for Pd(II), ^{1}A and ^{4}A for Co(II), ^{1}A for Cd(II), and ^{1}A and ^{3}A for Ni(II) complex. Figure (11-13) shows the most stable structure of these five complexes. The coordinate environment of the transition metal centers is different from each other, generally, the Cu(II), Co(II), and Ni(II) complexes are adopted octahedral geometry and the Pd(II) and Cd(II) complexes are adopted square planar and tetrahedral, respectively.

Table (4,5) illustrates the main structure parameters of the Cu(II), Pd(II), Co(II), Cd(II), and Ni(II) molecules of the most stable ground-state. For Cu(II) complex, the ground state is ^{2}A with Mulliken spin density of 0.47 (BP86) localized on the Cu, and the rest are distributed over the atoms coordinate to the Cu, mainly over S, Cl, N and O_3 atoms with values of 0.12, 0.15, 0.08 and 0.14, respectively. The expected typical octahedral geometry is distorted along the two-water molecule (z-axis) giving tetragonal geometry as shown in Figure(11-13). The bond lengths of the elongated Cu-O_1 and Cu-O_2 of 2.46 Å and 2.51 Å (BP86), respectively, compare to 2.46 Å, 1.96 Å, 2.27 Å, and 1.99 Å distances of Cu-S, Cu-N, Cu-Cl and Cu-O_3, respectively. The bond angles of O_1-M-O_2, S-M-Cl, and O_3-M-N of 164.01°, 91.64°, and 88.90°, respectively. These results are in good agreement with B3LYP calculations, for example, the M-O_1 within 0.07 Å, M-O_2 within 0.08 Å and O_1-M-O_2 within 0.41°. In a typical octahedric filed the $d_{x^2-y^2}$ and d_{z^2} orbitals are degenerated, however, in this molecule, the $d_{x^2-y^2}$ (HOMO orbital) is higher in energy than d_{z^2} by 0.39 eV (BP86). The possible ground state of Ni complex is ^{1}A or ^{3}A, our DFT calculations show that the ^{3}A is more stable than ^{1}A state by 0.15 eV with BP86, this is consistent with magnetic moment of 2.8 B.M and also with B3LYP predication where the ^{3}A now lies 0.79 eV lower in energy. The geometry of the Ni complex is octahedral, the Ni-O bond lengths of water molecules are symmetric with 2.22 Å calculated with BP86. The distances of Ni-S, Ni-Cl, Ni-N, and Ni-O_3 of 2.71 Å, 2.34 Å, 2.00 Å, and 2.01 Å, respectively. The Ni-S and Ni-Cl bond lengths are quite longer than the other by around 0.7 Å and 0.3 Å, respectively. The bond angles of O_1-M-O_2, S-M-Cl, and O_3-M-N are very similar to those of Cu(II) complex which are within around 1.5°. The ground state of the Co complex might be ^{2}A or ^{4}A states where d orbitals have one unpaired electron or three unpaired electrons, respectively. DFT calculations shows that the ^{2}A state is more stable than the ^{4}A by 0.11 eV. Therefore, ^{2}A is the ground state in agreement with the magnetic moment measurement suggesting low spin arrangement. The Mulliken spin density of 1.0 shows that the unpaired electron is completely localized on the cobalt center. The geometry of Co molecule adopted octahedral structure similar to Cu and Ni molecules. The two Co-O bond distances of water molecule of 2.31 Å and 2.32 Å (BP86), the distances of Co-S, Co-Cl, Co-N, and Co-O_3 of 2.28 Å, 2.30 Å, 1.88 Å, and 1.89 Å, respectively. The bond angles of O_1-M-O_2, S-M-Cl, and O_3-M-N are similar to that of other octahedral Cu(II) and Ni(II) molecules.

Figure(11-13) shows the most stable structure of Pd(II) complex with ^{1}A ground state, this state is more stable than alternative open-shell ^{3}A state by 1.5 eV calculated by BP86 functional. The most stable structure of Pd (II) molecule adopted square planar arrangement of the S, N, O, and Cl atoms of the two ligands. The bond distances of Pd-S, Pd-Cl, Pd-N, and Pd-O of 2.27 Å, 2.28 Å, 1.95 Å, and 1.97 Å, respectively. The ground state of Cd complex is clearly singlet as the four d orbitals are fully occupied. The Cd complex has the same four coordinates around the metal center to Pd (II) but they arranged in nearly tetrahedral fashion as shown in Figure11. The Cl-Cd-S angle is 107.02° similar to the angle of typical tetrahedral (109.5°), the Cl-Cd-O angle of 119.71° is quite diverged from the value of 109.5°, and the third angle of Cl-Cd-N is very different from the tetrahedral structure with value of 152.36° (PB86), these results are in agreement with B3LYP functional.

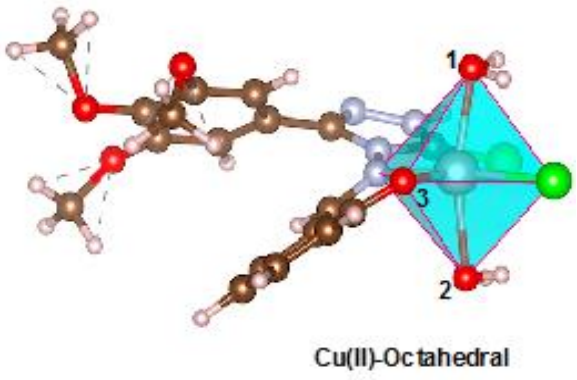

Fig 11. Structures of the CuL2 Octahedral complexes optimized by DFT. Color code: S in yellow, Cl in green, O in red, and N in light grey.

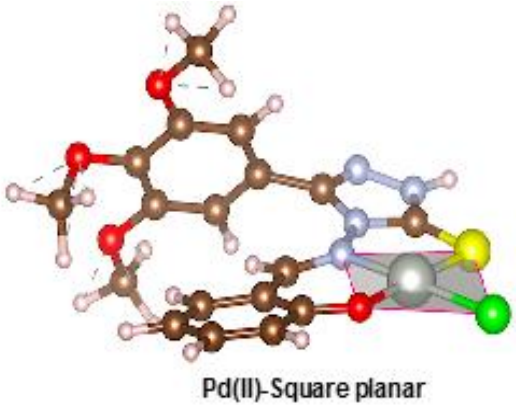

Fig 12. Structures of the complexes PdL2 Square planar optimized by DFT. Color code: S in yellow, Cl in green, O in red, and N in light grey.

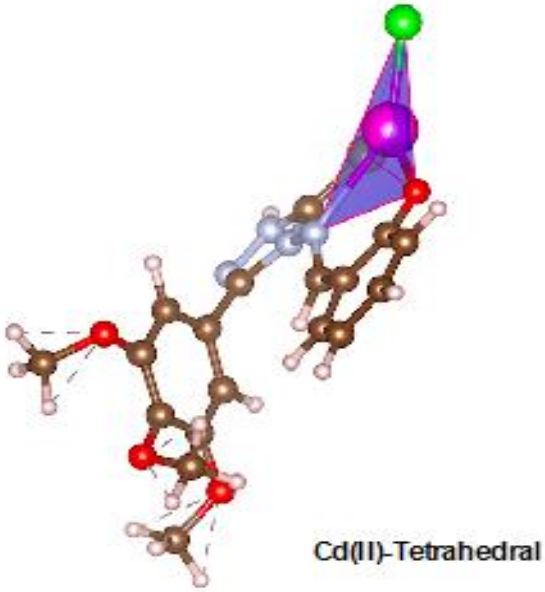

Fig 13. Structures of the CdL2 Tetrahedral complexes optimized by DFT. Color code: S in yellow, Cl in green, O in red, and N in light grey.

Table 4: structure parameters of Cu(II), Co(II), and Ni(II) complexes, bond length in Angstrom (Å) and bond angle in degree (°), the B3LYP values in parentheses, M refers to the transition metal.

Octahedral complexes			
Bonds	Cu(II) (^{2}A)	Ni(II) (^{3}A)	Co(II) (^{2}A)
M-O_1	2.46 (2.39)	2.22 (2.20)	2.31 (2.28)
M-O_2	2.51 (2.59)	2.22 (2.21)	2.32 (2.33)
M-O_3	1.99 (1.96)	2.01 (2.00)	1.89 (1.93)
M-S	2.46 (2.47)	2.71 (2.71)	1.88 (1.94)
M-N	1.96 (2.02)	2.00 (2.06)	1.88 (1.94)
M-Cl	2.27 (2.29)	2.34 (2.34)	2.30 (2.29)
O_1-M-O_2	164.01 (164.42)	162.36 (166.34)	166.02 (166.62
S-M-Cl	91.64 (92.10)	93.47 (93.75)	88.42 (90.58)
O_3-M-N	88.90 (87.83)	88.62 (86.64)	93.36 (90.06)

Table 5: structure parameters of Pd(II) and Cd(II) complexes, bond length in Angstrom (Å) and bond angle in degree (°), the B3LYP values in parentheses, M refers to the transition metal.

Square planer and tetrahedral complexes		
Bonds	Pd(II) (^{1}A)	Cd(II) (^{1}A)
M-O	1.97 (1.98)	2.23 (2.19)
M-S	2.27 (2.28)	2.92 (2.93)
M-N	1.95 (1.98)	2.75 (2.79)
M-Cl	2.28 (2.28)	2.38 (2.38)
Cl-M-O	89.15 (89.69)	119.71 (124.48)
Cl-M-N	---	152.36 (151.75)
Cl-M-S	88.71 (89.34)	107.02 (103.91)
O-M-N	93.11 (92.41)	75.50 (74.51)
S-M-N	88.98 (88.51)	67.57 (67.23)

TD-DFT calculations were carried out for further interpretation and understanding the electronic absorption spectra of all metal complexes. All TD-DFT calculations were applied to the most stable structure of the transition metal complexes using M06-L functional. The experimental spectra of Cu(II) complex show two bands, a broad band at 13333 cm^{-1} and another band at 23585 cm^{-1}. TD-DFT calculations show that the broad bad basically consist of three bands at 8761 cm^{-1}, 10309 cm^{-1}, and 13026 cm^{-1} belong to d-d transition ($d_{z^2} \rightarrow d_{x^2-y^2}$, $d_{xy} \rightarrow d_{x^2-y^2}$, and $d_{xz}, d_{yz} \rightarrow d_{x^2-y^2}$, respectively) [43]. The predicated band at 13026 cm^{-1} in very good agreement with the experimental value of 13333 cm^{-1}, this transition corresponding to $a_1 \rightarrow a_2$ transition as shown in Figure12, the a_1 orbital has significant contribution from chlorine. The second band is predicated at 23112 cm^{-1} in agreement with the experimental value of 23585 cm^{-1} have contributions from a large number of individual transitions, dominated by intra-ligand $\pi \rightarrow \pi^*$ transitions and L $\rightarrow$ Cu charge transfer. The experimental UV-Vis spectra of Ni complex show three peaks at 10405 cm^{-1}, 23255 cm^{-1}, and 33444 cm^{-1}, the types of these transitions are assigned with TD-DFT calculation. It predicts two peaks at 13597 cm^{-1} and 21970 cm^{-1} corresponding to d-d transition and one peak at 33613 cm^{-1} assigned to ligand to metal charge transfer [44].

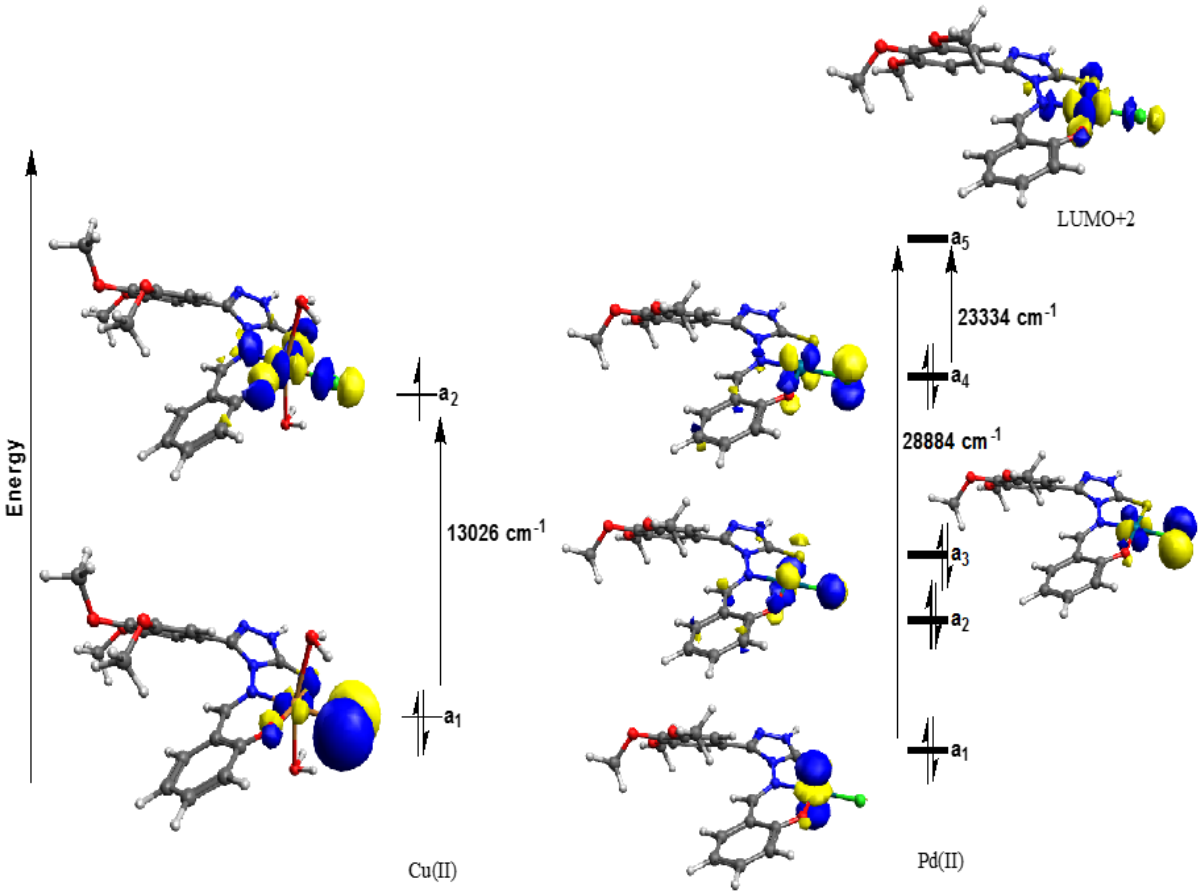

Fig 14. Frontier Kohn-Sham orbitals of Cu(II) and Pd(II) complexes (optimized with BP86 functional), only orbitals involve in d-d transition is shown.

For Pd(II) complex, the experimental electronic spectra show two peaks at 22727 cm^{-1} and 28571 cm^{-1}. Our TD-DFT calculation predicts a peak at 23334 cm^{-1} has contributions from several induvial transitions, dominated by $a_4 \rightarrow a_5$ (d-d) transition as shown in Figure 12 with significant contribution from Cl in orbital a_4. The second band is predicted to be 28884 cm^{-1}, this band consist mainly from two transitions [45]. The first transition from $a_1 \rightarrow a_5$ orbitals the second transition involve charge transfer between the metal center and the ligand, Figure (14).

3.6 Biological Activity Study

The Schiff base (L2) and its complexes are generally stable in the DMSO solvent so that used as a biological solvent media because of the stability of compounds in this solvent and its negative effect against studied bacteria, DMSO was selected as solvent media for the biological tests. The inhibition zone data for the entire complexes at concentration of (20 µg/ml) as compared with free ligand (L_2) should be discussed among the palladium (Π) complex has the highest inhibitory effect against the bacteria, the antibacterial activity of free ligand and its complexes showed the order:
PdL2 > CdL2 > CuL2 > CoL2 > NiL2 > L2 was found to be the ligand had the best effect [46].

Table 6. Diameters Inhibition Zone (mm) of the complexes against Bacteria and Fungi

Bacteria compound	C1	C2	C3	C4	C5
Candida albicans	10	10	10	25	13
Staphylococcus aureus	---	---	16	22	20
Staphylococcus epidermiddis	---	---	15	15	35
Escherichia coli	--	10	13	28	33
Klebsiella sp.	--	13	14	30	24

In general for the metal complexes showing antimicrobial activity the following five principal factors should be consider: The chelate effect, that is ligand that are bound to metal ions in a bi dentate fashion through NS and NO moiety of the ligands show higher antimicrobial efficiency compared with the complexes uni dentate respectively like pyridine.

However the total charge of the complexes in generally the antimicrobial activity decreases in the order cationic > neutral > anionic complex. Table 6 represents the inhibition zones (mm) for the Schiff base (L2) and its complexes against the bacteria and fungi in DMSO solvent as control. The free ligand exhibited low activity against all bacteria at around (5-10) mm and the PdL2 (C5) and CdL2 (C4) showed the greatest activity agains *E,Coli* and *Klepsiela Sp*, at (20-24) mm and (28-30) mm respectively. The concept of chelation theory for the lipophilic character in PdL2 and CdL2 complexes supported the high activity against the selected micro-organisms [47].

4. Conclusion

In the present research work, new Schiff base of (E)-2-(((3-mercapto-5-(3,4,5-trimethoxyphenyl)-4H-1,2,4-triazol-4-yl)imino)methyl)phenol (L1) has been synthesized by condensation reaction of 4-amino-5-(3,4,5trimethoxyphenyl)-4H-1,2,4-triazole-3-thiol with 2-hydroxybenzaldehyde. The new Schiff base (L) used as a ligand to synthesize a new complex with Co(II), Ni(II), Cu(II), Pd(II), and Cd(II) metal ions . New ligand and their complexes have been exanimated and Confirmed by (FT-IR), (UV-visible), (^{1}HNMR), (^{13}CNMR), (CHNS), thermal analysis (TG), atomic absorption flame (AAF), conductivity and Magnetic susceptibility. The results obtained from spectra, elemental analyses and the thermal analyses (TG-DSC) and Density functional theory (DFT) and TD-DFT calculations were screened for some selected complexes and the observed data indicated their stability and the expected chemical formula . The biological activity study for the Schiff base (L2) and its complexes was confirmed against two types of gram-positive and two negative-gram positive bacteria and the PdL2 and CdL2 complexes showed higher inhibition zones according diffusion method whereas the cOl,NiL2 and CuL2 showed medium activity in DMSO solution.

5. Acknowledgement

Authors are so thankful for the members of pharmacy faculty, Babylon University for facilitating the measurements of IR and UV spectra. As well as we are so grateful for the Mustansiriyah University, College of Science, Chemistry department for supporting the work through providing chemicals and measurements of molar conductance and magnetic susceptibility of the complexes.

6. References

1) Tozkoparan B, Küpeli E, Yeşilada E, Ertan M (2007), Bioorganic& medicinal chemistry;15 (4): 1808-14.
2) Sancak K, Ünver Y,Ünlüer D, Düğdü E, et al. (2012); Turkish Journal of Chemistry,36 (3): 457.
3) Ünver Y, Sancak K, Çelik F, Birinci E, Küçük M, Soylu S, et al. (2014), European journal of medicinal chemistry.84: 639-50.
4) Shalini K, Kumar N, Drabu S, Sharma PK. (2011), Beilstein journal of organic chemistry; 2(7): 668.
5) Küçükgüzel I, Tatar E, Küçükgüzel Ş G, Rollas S,De Clercq E. (2008), European journal of medicinal chemistry. 43 (2): 381-92.
6) Holla B S, Veerendra B, Shivananda M, Poojary. (2003), European journal of medicinal chemistry. 38 (7): 759-67.
7) Almasirad A, Tabatabai, S. Faizi M, Kebriaee A, Mehrabi N, Dalvandi A, et al. (2004), Bioorganic & medicinal chemistry letters.14 (24): 6057-9.
8) Palaska E, Şahin G, Kelicen P, Durlu NT, Altinok G. (2002). Il Farmaco. 57 (2): 101-7.
9) B.S. Holla, B. Veerendra, M.K. Shivananda, B. Poojary, (2003), Eur. J. Med. Chem. 38,759-767.
10) M.S. Karthikeyan, (2009), Eur. J. Med. Chem. 44 , 827-833.
11) S.G. Küçükgüzel, P. Çıkla-Süzgün, (2015) Eur. J. Med. Chem. 97, 830-870.
12) Al-Maydama H, Al-Ansi T, Jamil Y, Ali A (2008) , Ecl Quim 33 (3):29–42
13) Altalbawy, F. M. A., Mohamed, G. G., Abou El-Ela Sayed, M., & Mohamed, M. I. A. (2011), Monatshefte Für Chemie - Chemical Monthly, 143(1) , 79–89.
14) McCarrick R, Eltzroth M, Squattrito P (2000) , Inorg Chim Acta 311(1–2):95–105
15) Kasture, V. S., Katti, S. A., Mahajan,D., Wagh,R., Mohan,M.,&Kasture,S.B(2009) Pharmacologyonline , 1, 385-395.
16) Mahajan, S. K., RY, D. & Wagh, R. S. (2011). J. Pharma. Res, 4 (7), 2285-2287.
17) Setyawati, A. ,Wahyuningsih, T. D & Purwono, B.(2017).InAIP Conference Proceedings (1823,1, 20121).
18) Awad, A. A., Al-Hasani, R. A., & Yousif, E. A. (2015). Eur. J. Med. Chem. 38,759-767.
19) Bharty, M. K., Bharti, A., Chaurasia, R., Chaudhari, U. K., Kushawaha, S. K., Sonkar, P. K.,& Butcher, R. J. (2019).Polyhedron, 173, 114125.
20) Venugopala, K. N., Kandeel, M., Pillay, M., Deb, P. K., Abdallah, H. H., Mahomoodally, M. F., & Chopra, D. (2020). Antibiotics, 9 (9), 559.
21) Al-Shemary, R., Al-Khazraji, A. & Lateef, A, (2016), (IJSR), 5, 1787-1793.
22) ORCA, WIREs Comput . (2018) Mol .Sci. ,8, e1327.
23) Becke A. D.,(1993)., J. Chem. Phys., 98, 1372.
24) J. P. Perdew and Y. Wang, (1992), (Phys. Rev. B: Condens. Matter Mater. Phys., 45, 13245.
25) A. D. Becke, (1993), J. Chem. Phys., 98, 5648 – 5652.
26) P. J. Stephens, F. J. Devlin, C. F. Chabalowski, M. J. Frisch, (1994), J. Phys. Chem., 98, 11623 – 11627.
27) S. Grimme, S. Ehrlich, L. Goerigk, (2011) J. Comput. Chem., 32, 1456.
28) S. Grimme, J. Antony, S. Ehrlich, and H. Krieg, (2010). , J. Chem. Phys., 132, 154104.

29) F. Weigend and R. Ahlrichs, (2005) , Phys. Chem. Chem. Phys., 7, 3297.
30) F. Weigend and R. Ahlrichs, (2005) , Phys. Chem. Chem. Phys., 7, 3297–3305.
31) F. Weigend, (2006), Phys. Chem. 8, 1057,
32) P. Derivatives, W.A. El-sayed, and E.S. H. El-ashry, (2008), Arch. Pharm. Chem. Life Sci 341,307–313.
33) S. Menati, H. Amiri, B. Askari, M. Riahi, and G. Dini ,(2015), Comptes rendus - Chim. 1-10.
34) Ulusoy, N., Gürsoy, A., & Ötük, G. (2001). Il Farmaco , 56(12), 947-952.
35) Melaku M. and Ali M. (2018), Modern Chemistry Applications , 6 , (2) . 1000260.
36) Yu, M., Zhang, Y., Pan, Y. Q., & Wang, L. (2020). Inorganica Chimica Acta, 509, 119701.
37) N.N. Greenwood and A. Earnshaw; "Chemistry of the elements, A .Wiley intercince publication", 3rd edition, (1986).
38) W. A. Mahmoud and M. Ibraheem (2014) bag. sci.j. 11 (4) ,1519-1527
39) Tezgerevska, T., Rousset, E., Gable, R. W., Jameson, G. N., Sañudo, E. C., Starikova, A., & Boskovic, C. (2019). Dalton Transactions, 48 (31), 11674-11689.
40) Alothman, A. A., Albaqami, M. D., & Alshgari, R. A. (2021). J. of Molecular Structure, 1223.
41) Keypour, H., Shayesteh, M., Rezaeivala, M., Chalabian, F., Elerman, Y., & Buyukgungor, O. (2013).Journal of Molecular Structure,1032,62.
42) Yin C.-M.L., Zi-Ru Kong, Yang-Hui Wu, Cheng-Yun Ren, De-Hou Lü, Yu-Gang Xue, Hong-Fu,(1992)., Thermochimica acta, 204(2):251-260.
43) Y. Nishida and S. Kida ,(1979), Coordination Chemistry Reviews, 27, 275-298.
44) J. K. Bilyj, N. V. Silajew, and P. V. Bernhardt, (2021) , Dalton Trans., 50, 612.
45) B. So, D. Bust, S. Fuhrmann, M. Sierka, M. Peng, E-H. Heike, and L. Wondraczek,(2020) , J Am Ceram Soc.,103, 4214.
46) C. Holst-Hansen, N. Brünnner, (1998), MTT-cell proliferation assay, in: J.E. Celis (Ed.), Cell Biology: A Laboratory Handbook, Academic Press, San Diego, 16-18.
47) El-Gendy A.K., Aly N.M., Mahmoud F.H., Kenawy A. and El-Sebae A.K., (2010).The role of Vit C as antioxidant in protection of oxidative stress induced by Imidacloprid. Food Chem Toxicol, 48, 215– 221.